



Review

Advances on Dye-Sensitized Solar Cells (DSSCs) Nanostructures and Natural Colorants: A Review

José A. Castillo-Robles ¹, Enrique Rocha-Rangel ¹ , José A. Ramírez-de-León ², Frida C. Caballero-Rico ³ and Eddie N. Armendáriz-Mireles ^{1,*}

- ¹ Research Department, Universidad Politécnica de Victoria, Ciudad Victoria 87138, Tamaulipas, Mexico; a2183098001@alumnos.uat.edu.mx (J.A.C.-R.); erochar@upv.edu.mx (E.R.-R.)
- ² Academic Unit of Social Work and Sciences for Human Development, Autonomous University of Tamaulipas, Adolfo López Mateos University Center, Victoria City CP 87149, Mexico; ramirez@docentes.uat.edu.mx
- ³ Center of Excellence, Autonomous University of Tamaulipas, Adolfo López Mateos University Center, Victoria City CP 87149, Mexico; fcaballer@uat.edu.mx
- * Correspondence: earmendarizm@upv.edu.mx; Tel.: +52-834-171-11-00

Abstract: Human beings are attempting to take advantage of renewable natural resources by using solar cells. These devices take the sun's radiation and convert it into electrical energy. The issue with traditional silicon-based solar cells is their manufacturing costs and environmental problems. For this reason, alternatives have been developed within the solar cell field. One of these alternatives is the dye-sensitized solar cell (DSSC), also known as Grätzel solar cells. DSSCs are a type of solar cell that mimics photosynthesis. They have a photoanode, which is formed by a semiconductor film sensitized with a dye. Some of their advantages include low-cost manufacturing, eco-friendly materials use, and suitability for most environments. This review discusses four important aspects, with two related to the dye, which can be natural or synthetic. Herein, only natural dyes and their extraction methods were selected. On the other hand, this paper discusses the nanostructures used for DSSCs, the TiO₂ nanostructure being the most reported; it recently reached an efficiency level of 10.3%. Finally, a review on the novelties in DSSCs technology is presented, where it is observed that the use of Catrin protein (cow brain) shows 1.45% of efficiency, which is significantly lower if compared to Ag nanoparticles doped with graphene that report 9.9% efficiency.

Keywords: renewable energy capture; solar energy; Dye Sensitized Solar Cells natural dyes; solar cells; energy storage; nanostructures; efficiency



Citation: Castillo-Robles, J.A.; Rocha-Rangel, E.; Ramírez-de-León, J.A.; Caballero-Rico, F.C.; Armendáriz-Mireles, E.N. Advances on Dye-Sensitized Solar Cells (DSSCs) Nanostructures and Natural Colorants: A Review. *J. Compos. Sci.* **2021**, *5*, 288. <https://doi.org/10.3390/jcs5110288>

Academic Editors: Yiji Lu and Ke Tang

Received: 23 September 2021
Accepted: 18 October 2021
Published: 29 October 2021

Publisher's Note: MDPI stays neutral with regard to jurisdictional claims in published maps and institutional affiliations.



Copyright: © 2021 by the authors. Licensee MDPI, Basel, Switzerland. This article is an open access article distributed under the terms and conditions of the Creative Commons Attribution (CC BY) license (<https://creativecommons.org/licenses/by/4.0/>).

1. Introduction

The history of sensitized cells began with the pioneering work of Brian O'Regan and Michael Grätzel, on the promising applications of nanosized TiO₂ porous film electrodes in dye-sensitized solar cells (DSSC); these devices convert solar energy into electricity through the photoelectric effect [1]. The first devices worked with ruthenium-based dyes and their efficiencies were around 10% [2]. DSSCs are low cost to manufacture, eco-friendly, and are considered to have a high photon-to-electricity conversion efficiency, so they soon became an intense field of research.

DSSCs have great advantages compared to conventional silicon-based cells. Their construction is simpler as well as their maintenance; however, ruthenium (the predilect material) is a very scarce element in nature, leading to a very high price [3] in its acquisition and, therefore, it affects the overall price of the cell. Even if outputs are efficient, it is necessary to find a new material that addresses the requirements of low price and greater efficiency. For this reason, dye-sensitized solar cells (DSSCs) have been innovating. Thanks to numerous investigations, DSSCs have now reached an efficiency of approximately 13%, which has made them potential candidates to produce clean and renewable energy [4].

2. Dye-Sensitized Solar Cells (DSSCs)

DSSCs, also known as Grätzel solar cells, have a photoanode, formed by a metallic oxide (semiconductor), sensitized with a dye. Solar cells imitate the process seen in plant cells to produce energy (photosynthesis).

The basic components of a DSSC include a photoanode, a sensitizer, an electrolyte, and a counter electrode. Semiconductor nanostructures are used to develop the photoanode. Several nanostructures such as nanorods, nanotubes, nanowires, nanocones, nanosheets, or a combination of them, are manufactured on transparent conductive glass [5].

DSSCs are photonic devices that convert visible light into electricity and are based on a porous, thin film of a wide-bandgap semiconductor oxide modified by dye molecules. This type of film enhances light absorption due to its sponge-like characteristics and increased surface area. The nanocrystalline material plays an essential role in electron injection and transport, determining the performance of the DSSCs [6].

A typical DSSC consists of a transparent conductive oxide (TCO), semiconductor oxide, a dye sensitizer, an electrolyte, and a counter electrode. The working electrode is a nanoporous semiconductor oxide that is placed on a conducting glass, which is separated from the counter electrode by only a thin layer of electrolyte solution. The extension of the photoelectrode dye allows the collection of lower-energy photons. The dye is chemically absorbed on the semiconductor oxide surface. An ideal sensitizer should absorb a wide range of wavelengths and possess high thermal stability due to its strong binding to the semiconductor oxide [7]. The photoanode of a DSSC is typically constructed using a thick film (~10 μm) of TiO_2 or, less often, ZnO or SnO_2 nanoparticles. The TiO_2 film has a large inherent absorptive surface area for light scattering. One major challenge during the fabrication of DSSCs involves the matching of the material bandgaps and the structure design for each layer to give the maximum photoelectrochemical output and, thereby, the maximum conversion efficiency [8].

The typical architecture of a DSSC consists of a “sandwich” arrangement since it mainly has four parts, as shown in Figure 1: (a) photoanode (semiconductor oxide deposited on a transparent substrate); (b) light-sensitizing dye (dye molecules are anchored with the semiconductor to the photoanode); (c) electrolyte (redox couple); (d) counter electrode (generally, a thin film of platinum or carbon graphite). The principle of operation of a cell consists of the capture of photons of solar radiation by the dye. For this reason, the sensitizing molecule must have an intense absorption in the visible region of the electromagnetic spectrum where the radiative intensity of the sun is greater. Then, the dye, which is adsorbed on the photoelectrode (generally, nanostructured TiO_2), is excited by promoting an electron from its electron-filled level, called HOMO, to its first empty level, called LUMO [9,10]. The electron is then transferred to the mesoporous TiO_2 conduction band, which has a large surface area; this facilitates the injection of large amounts of charge carriers. This electron is then transferred to the transparent conductive oxide and transported to an external circuit until it reaches the counter electrode, which transfers the electron to the electrolyte so that the latter returns the electron to the dye—that is, regenerates it—and with this, the dye can absorb another photon from the medium and start the cycle again [11].

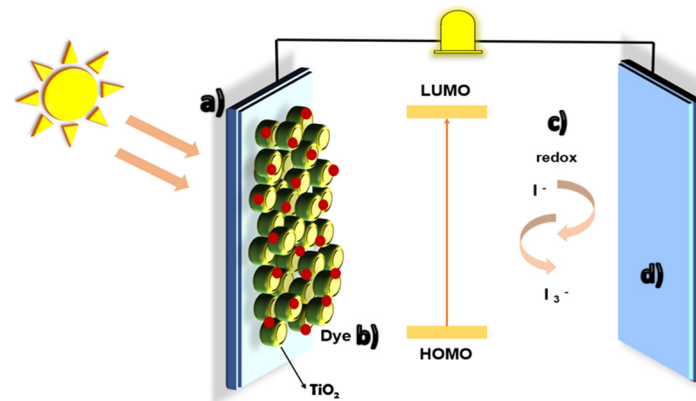


Figure 1. Typical components of a DSSC and functional mechanisms.

2.1. Natural Dye-Sensitized Solar Cells (DSSCs)

In a system, for converting pure, nonconventional solar energy into electricity, dye solar cells (DSSCs) promote the production of photovoltaic devices that offer high conversion efficiency at a low cost. The dye as a sensitizer plays an essential role in evaluating the performance of DSSCs. Natural dyes (organic dyes) have become a valid and common substitute for rare and expensive inorganic sensitizers due to their cost-effectiveness, high availability, and biodegradability. Various parts of plants such as fruits, leaves, flowers, and petals have been used as sensitizers over the years. The properties of these pigments, as well as some other parameters, improve the operational level of the DSSC [12].

Dyes are divided into organic dyes (natural dyes) and inorganic dyes. Inorganic dyes such as ruthenium (Ru) are currently known as the most important dyes for the production of highly efficient DSSCs. However, they are quite expensive and difficult to clean. To find an alternative to expensive and rare inorganic sensitizers, natural dyes are considered the most suitable substitutes. On the other hand, the main advantages of using natural pigments as sensitizers are low manufacturing costs, ease of manufacture, short payback period, flexibility, the availability of raw material supplies, and harmless risks. Furthermore, organic dyes comply with environmental protection and deliver excellent performance in diffuse and multicolor light options. Over the past decade, different parts of the plant, for example, the leaves, petals, and bark, have been studied as sensitizers. The nature and some other parameters of these pigments have delivered different levels of efficiency performance [13].

Pigmentation in plants results from the closed structure of pigments that sunlight controls, which change the wavelengths used by relationships. The pigment often has a wide range of light absorption in the visible region. The performance of the same sensitizing dye in DSSC was achieved under the management of fill factor (FF), energy conversion efficiency (η), open-circuit voltage (V_{oc}), and short-circuit current (J_{sc}). Many parts of a plant have been affected by differences in the dyes that belong to natural substances such as photosensitizers for DSSC [14]. Figure 2 shows the general molecular structure of anthocyanins.

Common pigments are (a) betalains, (b) carotenoids, (c) chlorophyll and (d) flavonoids such as anthocyanins.

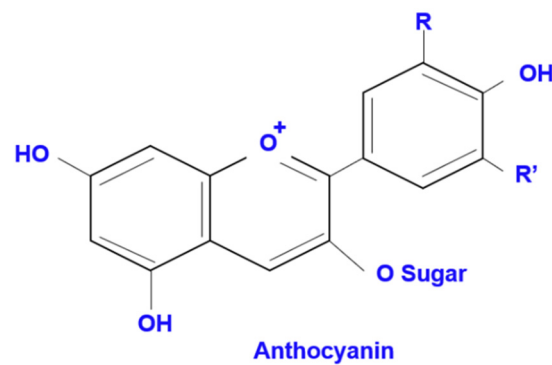


Figure 2. Illustration of anthocyanin molecule.

2.1.1. Flavonoids

Flavonoids are widely used plant pigments. More than 5000 natural flavonoids have been extracted from different plants and classified according to their chemical structure as follows: flavonoids, flavones, flavanones, isoflavones, catechins, anthocyanins, and chalcones. There are three classes of flavonoids: flavonoids (2-phenyl benzopyran), isoflavonoids (3-benzopyrans), and neoflavonoids (4-benzopyrans). Flavonoids contain a 15-carbon (C15)-based structure with two phenyl rings joined by three carbon bridges to form a third ring. The degree of oxidation of the phenyl ring (ring C) identifies the different colors of flavonoids. However, not all flavonoids can absorb visible light, although they have similar structures. Flavonoid molecules are characterized by having free electrons; this reduces the energy required to electronically excite LUMO, which means that visible light can supply energy to pigment molecules. Flavonoids are regularly found in fruits that attract feeding animals and spread fruit and flower seeds that attract pollinating insects. Many flavones and flavonols absorb the most concentrated radiation in the ultraviolet (UV) range and form special UV patterns on flowers that are visible to bees. They are also found in the leaves of many species, where they protect plants by filtering the sun's harmful ultraviolet rays. Flavanols, anthocyanins, and proanthocyanidins are the three main subcategories of flavonoid compounds [15].

2.1.2. Carotenoids

Carotenoids are organic pigments found in both chloroplasts and chromoplasts in plants and some other photosynthetic organisms, including some fungi and bacteria. Carotenoids perform two important functions in plants and algae: they absorb energy from light for use in photosynthesis, and they protect chlorophyll from light damage. Carotenoid pigments provide many flowers and fruits with the typical red, yellow and orange colors and a range of aromas derived from carotenoids. There are more than 600 known carotenoids, which fall into two categories—carotenes (pure hydrocarbons) and xanthophylls (containing oxygen). All carotenoids are tetraterpenoids, that is, they are made up of eight isoprene molecules and contain 40 carbon atoms. In general, carotenoids absorb wavelengths between 400 and 550 nanometers (purple to green light) [15,16]. Figure 3 shows the general molecular structure of (a) Carotenoids, (b) Flavonoids.

2.1.3. Chlorophyll

Chlorophyll (Chl) is the green color found in the leaves of most plants, cyanobacteria, and algae. There are six shades of dye that contain chlorophyll, the most common being Chla. Chlorophyll is a compound called a chelate, consisting of hydrogen, carbon, a large metal ion that binds to major molecules, and other elements such as oxygen and nitrogen. In photosynthesis, chlorophyll absorbs energy and converts carbon dioxide into carbohydrates and water into oxygen. This process converts solar energy into a form that plants can use. The molecular structure is composed of a chlorine ring with a Mg center, several chains, and small hydrocarbons, depending on the type of Chl [15].

Chlorophyll is the most important dye in image processing systems. Its function is to collect sunlight, convert solar energy into chemistry, and convert electrons. Chl consists of a group of more than 50 colors that contain lesions. Cl and its derivatives are included in the DSSC as paint diffusers due to their useful light transport properties. The most effective is Cl α (chl-methyltrans-32-carboxypyroformide). Chlorophyll has been reported to have the ability to drive four semiconductors to a TiO₂ and ZnO peak in different environments. Chlorophyll at 670 nm obtains moderate absorption with a spectacular field acting as a photographer in the visible light field [14,15].

Chlorophyll a is the main dye in plant matter, with a composition of C₅₅H₇₂O₅N₄Mg. It has bright green and blue leaves at 430 nm and 662 nm. Unlike chlorophyll a, the amount of chlorophyll b is C₅₅H₇₀O₆N₄Mg, with the substitution of methyl and CHO groups. It is bright blue in color with peaks at 453 nm and 642 nm [15].

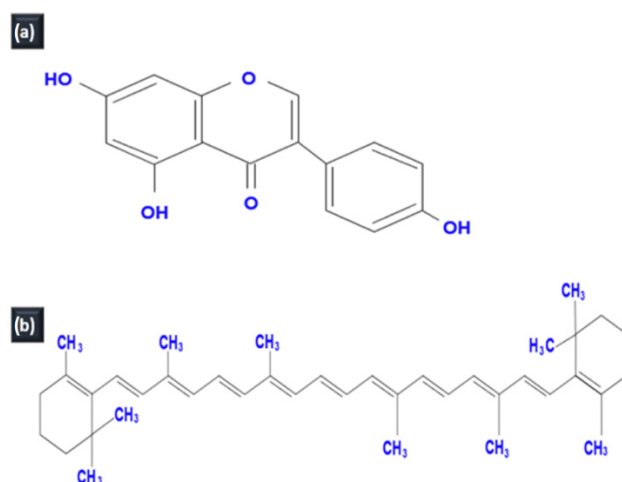


Figure 3. Illustration of the dyes reported in the literature of DSSC. (a) Carotenoids, (b) Flavonoids.

2.1.4. Natural Dyes in DSSCs Review

One of the most important points that has been given much emphasis in the research on dye-sensitized solar cells (DSSC) is the photosensitizers or dyes that are attached to a semiconductor. The function of photosensitizers is the absorption of light. The dyes used can have either a natural or synthetic origin. However, this review focuses on natural dyes.

Because it plays such an important role in the function of the DSSC and is the subject of study by a large number of researchers, a review of the literature on this topic is presented below in Table 1.

Table 1. Performances of DSSCs using natural dyes.

Dye Solution	Solvent	V _{oc} (V)	FF (%)	η (%)	Ref.
Purple cabbage and beetroot blend	Ethanol	0.43 V	60.0	0.38	[14]
80% beetroot + 20% spinach	Ethanol	386 mV	55.0	0.99	[15]
20% malabar spinach + 80% red spinach	Ethanol	385 mV	51.0	0.84	[16]
<i>Cassia fistula</i>	Ethanol	0.51 V	65.0	0.21	[17]
Spinach leaves	Acetone	0.59 V	58.0	0.17	
Purple cabbage	Oxygenated water	0.48 V	46.0	0.15	[18]
Onion	Oxygenated water	0.51 V	46.0	0.10	

Table 1. Cont.

Dye Solution	Solvent	V _{oc} (V)	FF (%)	η (%)	Ref.
<i>Cornelian cherry</i>	Acid solvent	0.39 V	31.0	0.98	[19]
<i>Cherry St. Lucia</i>		0.56 V	55.0	0.19	
Yellow jasmine berries	Ethanol	0.49 V	49.0	0.04	[20]
<i>Madder berries</i>		0.58 V	48.0	0.13	
<i>Crocus sativus</i>	-	0.43 V	48.0	0.51	
<i>Allium Cepa</i>	-	0.55 V	46.0	0.54	[21]
<i>Malva sylvestris</i>	-	0.49 V	42.0	0.45	
<i>Origanum vulgare</i>	-	0.43 V	47.0	0.51	
<i>Malaysian Areca Catechu</i>	Methanol, ethanol	0.539 V	72.0	0.07	[22]
Purple cabbage	Methanol, acetic acid	0.34 V	63.0	0.024	[23]
	Acetone	525 mV	51.0	0.10	
<i>Turmeric longa L.</i>	Ethanol	500 mV	29.0	0.12	[24]
	Methanol	568 mV	44.0	0.16	
<i>Berberis vulgaris</i>		0.571 V	60.0	-	
<i>Phytolacca americana</i>	Ethanol	0.570 V	65.0	-	[25]
<i>Jaboticaba</i>	Ethanol	0.41 V	29.0	0.13	[26]
<i>Alternanthera dentata</i>		0.54 V	56.0	0.15	
<i>Musa acuminata</i>	-	0.58 V	59.0	0.31	[27]
Papaya leaves	Ethanol	475 mV	56.0	0.07	[28]
<i>Hibiscus</i>	Methanol	0.24 V	50.0	0.034	
<i>Telang flower</i>	N-hexane	0.33 V	50.0	0.0183	[29]
<i>Musa acuminata bracts</i>	Ethanol, acetic acid	97 mV	8.88	0.097	[30]
<i>Mangosteen</i>	Methanol	0.64 V	56.0	0.38	[31]
60% turmeric + 40% red spinach	Ethanol	499 mV	50.0	1.07	[32]
<i>Pterocarpus Indicus Willd</i>	Methanol, ethanol, n-hexane	0.415 V	40.6	0.035	[33]

It should be mentioned that investigation outputs may vary from paper to paper, even if the same dyes were used. This is due to several factors such as the extraction method, the preparation of the solar cell, or simply the conditions in the place where the tests were performed.

On that note, articles [14,15] used beetroot as a base for the dye in a DSSC. However, their efficiencies were 0.1788% and 0.49%, respectively. The beetroot dye was not the main focus in either of the articles since each one uses a second dye to form the union. However, in the document [14], the use of purple cabbage as a second dye for their research is exposed and by combining it, an efficiency of 0.38% is obtained. On the other hand, the paper [15] presents spinach as a base for its second dye and reports an efficiency of 0.99% using 80% red dye and 20% green dye, in the combination of these two.

Similarly, references [16,18,32] used spinach as a base for the dye. However, as in the previous case, different results are presented. In the case of paper [16], the use of Malabar spinach and red spinach is reported, combining the dyes of these in a proportion of 20% and 80%, respectively; an efficiency of 0.84% is reported. On the other hand, the paper [18] does not present a combination of dyes, but the investigation of three dyes separately; the authors report the extraction of chlorophyll in spinach leaves using acetone

as a solvent and the extraction of anthocyanin from purple cabbage and onion peel. For this research, efficiencies of 0.17% for spinach, 0.151% for onion, and 0.104% for purple cabbage are reported. Continuing with the idea of spinach as a natural dye in the document [32], a combination of dyes is presented, within which is red spinach that, alone, gives an efficiency of 0.134%; as for the second dye used in this research, turmeric is used, which, alone, has an efficiency of 0.378%. Combining both in a proportion of 60% turmeric and 40% spinach, an efficiency of 1.079% is obtained.

In the reported literature, research was found in which not only a single dye is studied, but a certain amount of these are reviewed and compared to see their results and further expand the research on natural dyes. Such is the case of article [20], where research is reported on dyes of St. Lucie cherry and jasmine berries, yellow jasmine berries, and madder berries. This paper reports the use of ethanol as a solvent for the dyes and for use in solar cells with photoanodes formed by three TiO₂ layers, which were prepared using the coating method. Regarding the efficiency obtained, it is reported that cherry presents an efficiency of 0.19%, jasmine berry—0.04%, and madder berry presents an efficiency of 0.13%.

Furthermore, the article [21] reports the use of the solvent extraction method for the extraction of dyes, which was obtained from saffron, purple onion, mallow, and oregano. Regarding their low efficiency values from saffron 0.51%; mallow—0.45%; purple onion—0.54%; and 0.51% for oregano, authors report that these dyes contain carbonyl and hydroxyl groups, which allow them to bind to TiO₂ structures, and thus, improve electron transfer and energy conversion efficiency.

Dyes can commonly be obtained from different parts of plants, either from the fruit, the stems of the fruit peel, or the leaves. In the studies performed in the documents [27] and [28], the first research uses a dye extracted from the leaves of *Alternanthera dentata* and presents an efficiency of 0.15%. Investigators also employ the fruit of *Musa acuminata* and report an efficiency of 0.31%. It is worth mentioning that the dyes are applied as sensitizers of TiO₂. Moreover, reference [28] employs papaya leaves as a base for the sensitizer, obtaining an output efficiency of 0.07% with ethanol as a solvent. Following on from the previous idea where the dye is not extracted exclusively from the fruit, in paper [29], Hibiscus and Taleng flowers were used as sensitizer in DSSCs. In this paper, the focus is given to the colors obtained from the flowers, as the Hibiscus flower presents a red color while the Taleng flower presents a blue color. As for the efficiency of the dyes, it is reported that the Hibiscus flower presents an efficiency of 0.034%, while with the Taleng flower, an efficiency of 0.0183% is reported.

Further, different parts of a single plant can be used to generate dyes and compare the results. For example, paper [25] reports the use of barberry fruit and root as well as the use of the fruit and stem of the carmine herb. In this article, the extracts were used without any modification as purifiers or stabilizers. As for their efficiency, this research does not show such a result. The use of different solvents for the extraction of the dye is another technique employed. Therefore, article [24] reports turmeric longa L. as a base for the sensitizer. However, three types of solvents are used for the extraction of this. The first solvent is acetone, which results in an efficiency of 0.10%. Next is methanol, which presents an efficiency of 0.12%, and methanol exhibits the highest value with 0.16%. Finally, this research explored the optimization of some parameters such as pH of the solvent, loading period of the dye, and the percentage (%) of dye absorption on the TiO₂ film. When using different extraction methods on the same fruit, results can have different values. In reference [19], the authors report their extraction methods, which are acid solvent, mechanical extraction, and ultrasound-assisted extraction. Within these, there are more variants, presenting eight different results based on carmine cherry in the end. In this review, only the highest results obtained are presented. Therefore, the solvent extraction method, using methanol and citric acid, reported an efficiency of 0.98%. Article [17] reports the use of ethanol as a solvent for the extraction of dye from cassia fistula, where an

efficiency of 0.21% is reported. For this research, the flower of cassia fistula was reported to contain flavonoid pigments, mainly anthocyanin.

Some studies combine natural dyes and synthetic dyes to improve the overall efficiency of the DSSC. For example, paper [23] employed anthocyanin (purple cabbage) and obtained an efficiency of 0.024%. Then, anthocyanin and synthetic dye combination N719 resulted in an efficiency of 0.054%. The amount of dye used for each cell is 10 mL. Nevertheless, the first case uses 10 mL of purple cabbage, while the second uses 8 mL of purple cabbage and 2 mL of synthetic dye. The use of jaboticaba dye extracted by ethanol as a solvent is presented in the paper [26], in which it is reported that TiO₂ is used to improve the efficiency. Two methods are used to coat the photoanode: the first is the doctor blade method, which presents an efficiency with this dye of 0.08% and the second method reported is the spin coating method, which, with this dye, shows an efficiency of 0.13%.

Paper [22] presents a natural organic dye based on Malaysian Areca Catechu fruit. Herein, the authors evaluate the effects of several concentrations of chenodeoxycholic acid (CDCA) and solvent types to determine the photovoltaic efficiency of a DSSC. Then, the result from adding 1.5 mM CDCA at minute 0 is 0.068% efficiency. After 30 min, the efficiency of the dye lowers to 0.0118%. In paper [30], an efficiency of 0.097% is reported using *Musa acuminata* bracts as the basis for the sensitizer. Similarly, an efficient ZnO deposition at 3000 rpm, with diffusion of 0.05 mL of dye, is reported. Hence, the above-mentioned efficiency was achieved.

In some of the investigations carried out using natural dyes for DSSCs, the values obtained in terms of efficiency do not exceed the synthetic dyes; such is the case of the document [31], where the use of mangosteen as a base for the dye used is reported, which, by itself, presented an efficiency of 0.38%; to improve this value, different proportions chenodeoxycholic acid were added, and this was carried out to increase the performance of the DSSCs. The proportions that were added were 0.10, 0.50, 0.75, 1.00, 1.5, and 2.00 mM, the last one showing better results with 0.56% of efficiency.

Using *Pterocarpus Indicus* Willd as a base for the sensitizer, an efficiency of 0.035% was achieved, as mentioned in the paper [33], where TiO₂ was used as an electrode due to its thermal stability, and nontoxic, low manufacturing cost, among other characteristics. The conductive glass, which was coated with TiO₂, was immersed in the dye in three different duration treatments (12, 15, 18 h). It was found that the longer immersion duration results in a decrease in DSSC efficiency; a light intensity of 100 and 150 mW/cm² was also applied in each of the cases and it was found that the increase in light intensity illumination increases the efficiency.

It has been found that performance of DSSC could be enhanced by choosing the proper extraction method. Table 2 shows different extraction approaches.

Table 2. Extraction methods of natural dyes for DSSC review.

Natural Sensitizers	Tools	Medium	FF (%)	V _{oc} (V)	H (%)	Ref.
<i>Jatropha</i> leaves	Ethanol, acid citrate, distilled water	Ethanol, acid citrate, distilled water	-	3.5 mV	5.53 × 10 ⁻⁶	[34]
<i>Chrysanthemum purple</i>			-	22.5 mV	1.91 × 10 ⁻³	
Combination of purple cabbage, spinach leaf, turmeric stalk	Scissors, biker, ultrasonic cleaner, centrifuge	Ethanol	68.0	0.53 V	0.602	[35]
<i>Podophyllum Schott</i>	scissors, distilled water, mortar and pestle, centrifuge, centrifuge	Ethanol	44.0	0.86 V	0.308	[36]
Blueberries	Distilled water, mortar, and pestle, Whatman filter, micro-oven, analytical balance	Ethanol, acetic acid, water, and ethyl alcohol	-	-	24.62 × 10 ⁻¹²	[37]
Grenada			-	-	15.75 × 10 ⁻¹²	
Avocado peel			-	-	48.25 × 10 ⁻¹²	

Table 2. Cont.

Natural Sensitizers	Tools	Medium	FF (%)	V _{oc} (V)	H (%)	Ref.			
Grenada	Mortar, net (filter), filter(paper)	-	20.90	304 mV	0.20	[38]			
Sage flower	Oven, mortar, stirrer	Methanol	40.0	461 mV	0.152	[39]			
<i>Spathodea</i>			41.0	525 mV	0.217				
<i>Ipomoea Batatas L.</i>	Mortar, scale, magnetic stirrer, and Whatman filter n42	Methanol, distilled water, and acetic acid	-	0.19 mV	0.019	[40]			
30% beetroot, 50% lemon leaves, and 20% spinach leaves	Knife, pestle and mortar, Whatman filter, oven	Ethanol	-	0.65 V	0.013	[41]			
50% Pomegranate, 30% Beetroot, and 20% Spinach Leaves			-	0.47 V	0.03				
Mixture of maqui and blackberry (<i>Aristotelia chilensis</i> and <i>Rubus glaucus</i>).	Oven, grinder, strainer Whatman filter n	Distilled water	59.0	0.459 V	0.29	[42]			
Raspberry	-	Water	38.90	0.21 V	0.128	[43]			
Grenada	Distilled water, mortar, filter	Ethanol and distilled water	65.0	0.52 V	0.115	[44]			
<i>Beta vulgaris</i>	Knife, stirrer, filter	Acetone	53.0	0.86 V	2.73	[45]			
<i>Syzygium comini</i>			63.8	0.47 V	1.05				
Pandan leaves			44.0	0.48 V	0.57				
Spinach leaves			50.0	0.47 V	0.44				
Sawi	Distilled water, knife, filter	Ethanol	50.0	0.46 V	0.40	[46]			
<i>Sargassum</i>			47.95	0.404	0.73				
<i>Garcilaria</i>			48.88	0.442	0.86				
<i>Enteromorpha</i>			Oven-dried at 42 °C, and powdered	Ethanol/Water	50.21		0.473	1.05	[47]
<i>Malva verticillata</i>					55.39		0.542	1.70	
<i>Suaeda aegyptiaca</i>					51.65		0.491	1.16	
Grapes	Mortar, centrifuge and filter	Ethanol	62.0	0.39 V	1.46	[48]			
Spinach			64.0	0.33 V	1.64				
Papaya peel	Furnace, stirrer, centrifuge, filter, ultrasonic equipment	Hexane	69.5	0.576 V	0.093	[49]			
Microalga <i>Scenedesmus obliquus</i>		Methanol	69.0	0.587 V	0.64				
<i>Citrus paradisi</i>		29.0	0.323 V	0.028					
<i>Citrus sinensis</i>		Distilled water, oven, mortar and pestle, filter	Ethanol	30.4	0.285 V		0.013		
<i>Citrus limonum</i>				28.0	0.291 V		0.004		
<i>Citrus tangelo</i>	26.0	0.307 V	0.022						
Prickly pear pulp	Distilled water, oven, mortar, filter	Ethanol	85.0	0.56 V	0.56	[51]			
Tomato	Knife, filter, rotary evaporator	N-hexane	37.0	0.14 V	0.03	[52]			

In the document [34], the sensitizer is extracted from jatropha and purple chrysanthemum leaves, obtaining an efficiency of 5.53×10^{-6} in jatropha leaves and 1.91×10^{-3} in purple chrysanthemum. For this research, the process that was carried out was to cut the leaves approximately 2 cm × 2 cm. Then, they were washed with distilled water and dried in an oven at 40 °C; after, they were crushed in a mortar to make powder. These powders were dissolved in ethanol, acid citrate, and distilled water (10 g of powder, 10 mL of ethanol, 2 mL of acid citrate, and 8 mL of distilled water), and stirred with a magnetic stirrer at 60 °C for 30 min. The solution was left for 24 h at room temperature without light, then filtered with a Whatman filter (No. 42) to remove the residues.

The use of a combination of dyes as possible sensitizers is another point of research. For example, paper [35] mixed dyes based on purple cabbage, spinach leaf, and turmeric stem. Then, they were studied separately; at the same time, a mixed dye based on purple cabbage, spinach leaf, turmeric stem was examined. An efficiency of 0.602% was reported, this being the efficiency of the mixed dye and the highest. As for the extraction, the species were cut into small pieces and crushed in a mortar, then placed in an ultrasonic cleaner for 15 min; after, the mixture was segregated with a centrifuge at 2500 rpm for 30 min.

In the case of chlorophyll, the extraction of *Podophyllum Schott* leaves is reported in document [36], where 0.308% efficiency is obtained. For the extraction of this dye, the leaves were washed with distilled water and cut into small pieces. The pieces were dried at room temperature for 1–2 days, and then, were crushed into powder. The powder was dissolved in ethanol for 14 days at room temperature without light. The chlorophyll solvent was separated by centrifugation at 4500 rpm for 10 min and filtered using Whatman paper under vacuum conditions.

In contrast, in paper [37], the study of three different dyes extracted from blueberries, pomegranates, and avocado peel is presented. Regarding the efficiencies recorded in this research, it can be said that they were relatively low compared to other works; avocado peel showed an efficiency of $48.25 \times 10^{-12}\%$, blueberries showed an efficiency of $24.62 \times 10^{-12}\%$ and finally, pomegranate showed an efficiency of $15.75 \times 10^{-12}\%$. For the extraction method, 10 g of blueberries and pomegranates were each taken and washed with distilled water; then, they were crushed into small pieces using a mortar, immersed in ethanol/acetic acid/water in a ratio of 25:4:21 by volume, and finally, filtered with Whatman paper. As for the avocado, the peel was crushed to a fine powder using a mortar; then, 5 g of this powder was immersed in 25 mL of ethyl alcohol, left at room temperature without light, and filtered with Whatman paper.

One of the most frequently repeated dye bases in this review is pomegranate, as shown in papers [38,41,44]. In the first case, paper [38] obtained an efficiency of 0.20%. In this research, anthocyanin is used as a sensitizer; the pomegranate was washed to reduce the powder particles, and the juice was extracted by manual grinding and filtered through a net and filter paper to obtain a clear dye solution. On the other hand, in paper [41], different tests were carried out with different mixtures of dyes using pomegranate (PG), beetroot (BR), lemon leaves (LM), and spinach leaves (SC) as bases; in this study, the dyes that stood out the most were, firstly, the dye composed of LM 50%/BR 30%/SC 20%, which gave an efficiency of 0.013%, and secondly, the dye composed of BR 30%/PG 50%/SC 20%, which gave an efficiency of 0.03%. As for the extraction method, the pomegranate and beetroot were cut into slices and ground, then filtered; 60 mL of extract was taken from each and was combined with 30 mL of ethanol, boiled for 30 min and filtered again. In another instance, lemon and spinach were oven-dried at 60 °C for 24 h; 2 g of dried leaves of each were immersed in 20 mL of ethanol at room temperature and no light for a day, and lastly, filtered. Finally, in paper [44], where the basis for the dye of this study an efficiency of 0.115% was reported. For preparation of the dye, it was washed several times with distilled water to remove dust and other impurities. The dye was obtained using a maceration technique. The crushed fruit was immersed in the solvent (100 mL of ethanol and 50 mL of distilled water) for 24 h and, finally, filtered.

In paper [39], the use of sage and spathose flowers was reported as a base for the natural dye used as a sensitizer in DSSC. In this research, an efficiency of 0.152% is reported for the dye based on sage flowers. In contrast, spathose flower reported an efficiency of 0.217%. For preparation of the dye, the flowers were dried in an oven at a temperature of 323 K or 58.85 °C; then, the dried flowers were crushed to obtain a powder and dissolved in methanol. The solution was placed in a shaker for two days.

The use of *Ipomoea batatas* dye as a sensitizer for DSSC was reported for the first time. The results delivered an efficiency of 0.0193% [40]. The preparation of this dye followed this methodology: 15 g of sweet potatoes were taken with a mixture of 45 mL of methanol

solution, distilled water, and acetic acid; the dye was stirred with a magnetic stirrer at 450 rpm for 1 h and then, a Whatman No. 42 filter was used for filtering.

A study of a mixed dye of maqui and blackberry was carried out based on the amount of anthocyanin [42]. Herein, several studies were performed, but one of them used an anthocyanin concentration of 750 mg/L and reported an efficiency of 0.194%. On the other hand, a concentration of anthocyanin 1500 mg/L showed an efficiency of 0.290%. To obtain this dye, the fruits mentioned above were dried at 45 °C until constant weight, ground, and sieved. Then, 0.5 g of dried fruits were macerated in 5 mL of distilled water, and their solid residues were filtered with a Whatman No. 1 filter; finally, they were protected from light exposure and stored at 5 °C.

Article [43] achieves an efficiency of 0.128% by using raspberry as the base for the sensitizer. The dye preparation method was the following: 12 raspberry fruits were immersed in 20 mL of water for one day. Then, the solution was filtered to obtain a clear red liquid, which is the anthocyanin dye, without further purification. This work did not use solvents or other techniques besides letting the fruit sit in the water.

In this work [45], *Beta vulgaris* and *Syzygium cumin* were used as the base for the dye. After performing tests, the authors reported 1.05% efficiency for *Syzygium* and 2.73% for *Beta vulgaris*. The preparation methods of these dyes included the following steps: the species were cut into small pieces and soaked in 150 mL of acetone, and stirred for 12 h at room temperature. The resulting solution was filtered with filter paper, and the filtrate was washed several times with hexane, protected from direct light exposure, and stored in a refrigerator at 5 °C.

Reference [51] presents an innovative approach where authors employ prickly pear pulp as a base for the dye, obtaining an output efficiency of 0.56%. The preparation method used 50 g of prickly pear pulp. However, it is worth mentioning that the prickly pear was completely ripe. For developing the dye, 50 mL of ethanol was shaken for two hours at room temperature. Then, it was transferred to airtight containers and covered with aluminum foil for protection against light. Finally, it was stored in the refrigerator at 3 °C.

Occasionally, dyes based on species originating in certain specific places are used. Nevertheless, some studies use commonly known species. In paper [52], common fruits and vegetables (orange, carrot, and tomatoes) are used as a base for the dye. The preparation method begins by cutting the species into small cubes. After that, carotenoid dyes are dissolved in n-hexane and maintained for 24 h, and then filtered. Next, the dye was evaporated using a rotary evaporator to obtain more concentrated solutions. In terms of efficiency, tomato-based dye yielded 0.03%, orange-based dye reached 0.02%, and carrot-based dye achieved 0.009%.

The document [50] presents a study based on citrus fruits where grapefruit (*Citrus paradisi*), orange (*Citrus sinensis*), lemon (*Citrus limonum*), and mandarin (*Citrus tangerina*) are used as a base for dyes. Concerning efficiency, the highest value achieved was grapefruit-based dye (0.028%), and the lowest result was the lemon-based dye (0.004%). Preparation included washing the peels of these citrus fruits several times in distilled water and drying them in a vacuum oven at 60 °C. After that, peels were crushed into powder. The next step was to dissolve 5 g of powder in 250 mL of ethanol and leave it for 48 h at room temperature. Finally, the solutions were filtered and protected against light exposure.

The research conducted on a combination of papaya peel dye and microalgae *Scenedesmus obliquus* is presented in the paper [49]. In this work, dyes are studied individually and mixed. The mixed dye obtained higher efficiency in this study, with 0.134%. For the preparation, papaya peel dye was dried in an oven for 24 h at 50 °C. Then, 5 g of dry skin were mixed with 50 mL of hexane. Next, the mixture was shaken for 48 h and later, centrifuged at 4000 rpm for 5 min at 10 °C. After that, it was filtered using a nylon membrane and dried with a rotary evaporator. As for the microalgae dye, 4 g of microalgae biomass was taken and soaked in 10 mL of methanol; then, it was centrifuged at 4500 rpm for 10 min at 4 °C, sonicated for two hours and left overnight with gentle agitation and protected from light; finally, it was filtered.

The study of dyes based on pandan leaves, spinach leaves, and sawi leaves is shown in paper [46], where the way of extraction of the dyes started by taking 20 g of each type of fresh leaf with distilled water, then rinsed with ethanol and cut into small pieces. The pieces were deposited in 200 mL of ethanol and left overnight in the dark. Finally, they were filtered to remove excess residues. With this procedure, it was possible to obtain 0.57% efficiency in pandan leaves, 0.44% efficiency in spinach leaves, and 0.40% efficiency in sawi leaves.

To conclude this section, the document [48] was reviewed, where it is reported the use of grapes and spinach as a base for the sensitizers; it was shown that the grape-based dye has an efficiency of 1.4609%, while the spinach-based dye has an efficiency of 1.6424%. In addition, the extraction method followed to obtain these dyes began by cleaning and crushing in a mortar and then depositing in 30 mL of ethanol, then the solution was centrifuged and filtered

2.1.5. Recent New Ideas on Natural Dyes for DSSCs

Nowadays, dye origin is a relevant factor, whether it is synthetic, natural, or combined (Table 3). This section presents recent developments in dyes. It has been found that performance of DSSC could be enhanced by choosing the proper extraction method. Table 2 shows different extraction approaches.

Table 3. New dyes for DSSC.

New Dye	Type	FF (%)	V _{oc} (%)	η (%)	Ref.
Hybrid dye (synthetic dye DN-F01 and natural dye of turmeric and black rice shown)	0.125%DN-F01+blackrice	56.9	364 mV	0.996	[53]
	0.5%DN-F01+blackrice	57.9	394 mV	1.014	
	1%DN-F01+blackrice	65.6	378 mV	1.065	
D-π-A organic dyes for DSSC based on dibenzo [1,6] naphthyridine and donors such as trimethoxy, methoxy, dimethylamino	dibenzo [1,6] naphthyridine group Trimethoxy	74.0	0.642 V	3.22	[54]
	dibenzo [1,6] naphthyridine group Methoxy	69.0	0.621 V	2.13	
	dibenzo [1,6] naphthyridine group Dimethylamino	74.0	0.648 V	5.02	
MR1, MR3, and MR4 metal-free organic dyes containing N, N-diethylaniline as donor group, rhodanine-3-acetic acid as acceptor group separated by thiophene as spacer	MR1	67.2	0.538 V	3.51	[55]
	MR3	68.9	0.584 V	6.56	
	MR4	69.5	0.577 V	6.32	
Hemicyanine-based sensitizers having N-diethyl aniline as primary donor and hydroxy or alkoxy as auxiliary donors.	MA3	51.0	0.698 V	4.39	[56]
	MA4	53.0	0.696 V	4.62	
	MA5	53.0	0.712 V	4.97	
Azo dyes have different conjugation lengths and different donor residues, based on 5-amino isophthalic acid.	1b	47.5	0.910 V	0.14	[57]
	2b	50.0	0.911 V	0.19	
	3b	50.01	0.912 V	0.22	
Difunctionalized dyes based on two different scaffolds: p-tert-butylcalix[4] rene or isophthalic acid	AT-L	63.7	0.568 V	4.75	[58]
	Cx-2-AT-L	60.3	0.645 V	5.20	
	Ft-2-AT-L	70.7	0.566 V	3.50	
Development of three highly stiff quinoxaline-based dyes	LY01	64.99	0.61 V	5.06	[59]
	LY02	65.25	0.66 V	6.08	
	LY03	53.90	0.91 V	7.04	

Reference [53] exhibits a combination of two dyes to create a hybrid one based on turmeric and black rice (anthocyanin) and a DN-F0 synthetic dye. For this research, an FTO glass with TiO_2 was used as the electrode; this was carried out with the method of rotational coating. On the other hand, FTO glass with platinum paste was used as the counter electrode. The tests that were carried out were divided into testing the rice by itself, testing the synthetic dye by itself, and testing the combination of both. The best results were obtained when testing the synthetic dye without any complement, reaching 2.018% efficiency; as for the hybrid dye, the highest efficiency recorded was 1.065%.

In contrast, reference [54] reports organic dyes based on dibenzo naphthyridine and, as electron donors, trimethoxy, methoxy and dimethylamino. In this work, the authors state that the organic dye with dimethylamino showed a better intramolecular charge transfer in the theoretical calculations. Moreover, it showed a higher and red-shifted absorption due to its electron-donating capacity. On the other hand, this dye shows the highest efficiency in this work with 5.02%.

The use of metal-free organic dyes is presented in paper [55]. In this study, four dyes (MR1, MR2, MR3, and MR4) are investigated and efficiencies of 3.51%, 2.58%, 6.56%, and 6.32%, respectively, are presented. They also report that the photophysical behavior of the composites shows sensitivity to structural modification and the solvent environment and shows a good correlation with the theoretical absorption obtained by TD-DFT calculation. It should be noted that these compounds are based on hemicyanine, with N-diethyl aniline as the primary donor and hydroxy or alkoxy as the auxiliary donor.

Article [56] describes five hemocyanin-based sensitizers, with N-diethyl aniline as the primary donor and hydroxy or alkoxy as auxiliary donor; these were synthesized to establish a correlation between the amphiphilic nature of the sensitizer and charge recombination. These five sensitizers correspond to MA1, MA2, MA3, MA4, and MA5, and their efficiency values correspond to 3.4%, 4.17%, 4.39%, 4.62%, and 4.97%, respectively.

Azobenzene units were used as the π -spacer part to extend the conjugation range of connecting the donor unit to the acceptor [57]. Herein, the design and synthesis of a series of azo dyes possessing different conjugation lengths are reported. In this study, investigators employed six dyes: 1–3a and 1–3b. The highest efficiency values are attributed to 3a and 3b, with 0.21% and 0.22%, respectively. On the other hand, they report that the conjugation of extended π and the included donor moiety with hydroxyl caused a red shift in the absorption wavelength and increased absorption intensity.

Paper [59] reports the development of three highly rigid quinoxaline-based dyes (LY01, LY02, and LY03). In this study, investigators tested their performances and showed that the LY03 dye had the best efficiency of this group with 7.4%. They also state that the improvement of the molecular rigidity of the sensitizer and the incorporation of long alkyl chains in an acceptor and an auxiliary donor is a way to prevent the compensation effect.

Finally, reference [58] reports the development of a DSSC with difunctionalized dyes, which are based on isophthalic acid or 4-tert-butylcalixarene as a framework and N-N-dialkylaniline as electro donor connected to thiophene as π -spacer. For this research, three cases are presented to study (AT-L, Cx-2-AT-L, and Ft-2-AT-L), and after performing the corresponding tests, it is concluded that the Cx-2-AT-L case is the one that shows the highest efficiency with 5.20%. Similarly, that calix-arene based dye has the best light-harvesting ability. On the other hand, a blocking layer between TiO_2 and electrolyte is reported, which leads to better suppression of the return electron transfer of the injected electrons.

2.2. Nanostructures Reported on DSSC

One of the methods currently used to improve the efficiency of DSSCs is nanostructures. Nanostructures possess different properties depending on their structure. For this reason, it can potentially benefit the DSSCs if the appropriate walls are achieved. TiO_2 is one of the most reported nanostructures, and it undergoes several processes to improve efficiency. Nevertheless, it is worth mentioning that other particles are currently used and

have comparable results with TiO₂. The following section summarizes the literature on nanoparticles in DSSCs.

2.2.1. Nanostructures TiO₂

At present, one of the particles most commonly used in DSSCs as a semiconductor is titanium oxide (TiO₂). TiO₂ nanostructures have had good results and improvements. As a result, several studies have been performed (Table 4). Regarding the subject mentioned above, this section exclusively reviews TiO₂ particles in DSSC technology.

Table 4. Nanostructured TiO₂ and techniques found in recent literature.

Idea	Particle	Technique	Structure	η (%)	Ref.
Investigate the correlation between the properties of the nanostructure to obtain the optimum parameter for best performance	TiO ₂	Sol-gel	-	-	[3]
The Au/TiO ₂ /SiO ₂ core-shell characteristics and their effects on DSSC performance were investigated.	TiO ₂	Doctor blading	-	0.016	[5]
Presents a hetero-seed mediated method to synthesize ZnO/TiO ₂ multimode nanocomposites based on ZnO and TiO ₂ nanowires.	TiO ₂	Hydrothermal	Nanowires	3.10	[10]
In this work, TiO ₂ nanotubes were prepared from TiO ₂ nanoparticles under the influence of 10 M NaOH.	TiO ₂	Solvothermal	Nanotubes	7.20	[11]
Photoanodes composed of a bottom layer of common TiO ₂ nanoparticles and as a top layer one- and three-dimensional TiO ₂ nanostructures.	TiO ₂	Doctor blading	Nanowires	9.9	[60]
			Core-shell microspheres	9.2	
			Nanorods	8.27	
			Nanowires	8.04	
New method to prepare photoelectrodes incorporating locally ordered 3D-IO TiO ₂ nanostructures.	TiO ₂	New method	Inverse Opal 3D	10.35	[61]
3D hierarchical structure of TNS (TiO ₂ nanosheet spheres) as light scattering layer and a P25/TNR(TiO ₂ nanorod) structure as bottom layer	TiO ₂	Hydrothermal	3D nanosheet sphere	5.99	[62]
TiO ₂ nanostructures with two different dopants, sodium and yeast, to improve the efficiency of DSSCs	TiO ₂	Hydrothermal	Nano-corals/nanorods	2.31	[12]
Sodium-doped TiO ₂ nanostructures and yeast.	TiO ₂	Hydrothermal	Nanorods/nanoflowers	2.40	[13]

These investigations range from using doping in TiO₂ nanostructures to trying to find the optimal parameters of these nanostructures, as in paper [3], where authors report the use of the sol-gel technique, using TiO₂ particles to find an optimal parameter for better performance of DSSCs. Nevertheless, and despite expressing different results in their tests, their efficiency is not reported.

On the other hand, paper [5] modifies the photoanode of a DSSC by adding Au/TiO₂/SiO₂. The authors report an efficiency of 0.016% and an increase of 92.9% compared to an unmodified photoanode (TiO₂); this result was achieved by using the doctor blading technique and adding 90 mL of SiO₂. However, if a smaller amount is added, the core is partially uncovered; if a larger amount is added, there is an agglomeration.

In reference [10], authors achieve multipod nanostructures based on ZnO and TiO₂ nanowires, reporting an efficiency of 3.10%; this is achieved thanks to a hydrothermal method and using TiO₂ nanoparticles as a nucleated site for the growth of ZnO nanowires. These nanowires, scattered from TiO₂ nanoparticles, form ZnO/TiO₂ multipodnanostructures.

Modifying TiO₂ particles can offer efficient results, such as the case of the study presented in paper [11], which reports the use of sodium hydroxide (NaOH) and a solvothermal method to achieve a TiO₂ nanotube nanostructure, reaching an efficiency of 7.20%. It was found that the surface area of the nanotubes was larger compared to the initial nanoparticles, and bimodal pore distributions were observed.

One of the research papers that presents better results for efficiency is [60]. This article reports the use of a double-layer photoanode, where the bottom layer is TiO₂ nanoparticles and the top layer is TiO₂ nanostructures. Within these nanostructures, nanowires and microspheres are shown, these being the ones that showed a higher efficiency; the first showed an efficiency of 9.9% and the second of 9.2%. With this bilayer configuration, the authors achieved the formation of TiO₂ networks that are well connected between their intermediate layers; this, in turn, has shown synergistic effects in the control of light and electron transfer within the photoanodes.

Paper [61] is an innovative approach that achieved 10.35% efficiency. The authors created a new method to synthesize 3D inverse opal TiO₂ mesoporous nanostructures. This work used an organic dye (YKP88) and ruthenium complex dye N719. Then, the authors reported that the addition of nanostructures increased the efficiency of the organic dye by 17%. Likewise, the second dye increase 12% compared to a conventional DSSC.

In paper [62], the hydrothermal method generated a cell efficiency of 5.99% thanks to a 3D hierarchical structure of TNS (TiO₂ nanosheet spheres). This is applied as a light scattering layer for the photoanode; likewise, for the latter, a P25/TNR structure (TiO₂ nanorods) is applied as a bottom layer. It is also reported that this double layer structure exhibits excellent light harvesting.

At the beginning of this section, it was mentioned that one of the methods to improve efficiency is to use dopants in the TiO₂ particles; this can be seen in references [12,13]. In both cases, the hydrothermal method is used, and sodium and yeast are used as dopants. The main difference between them is shown in the nanostructures obtained (Figure 4). In article [12], nano-corals and nanorods are reported to achieve an efficiency of 2.31%. On the other hand, in paper [13], the appearance of nanorods and nanoflowers as TiO₂ nanostructures is reported, where they obtain an efficiency of 2.40%.

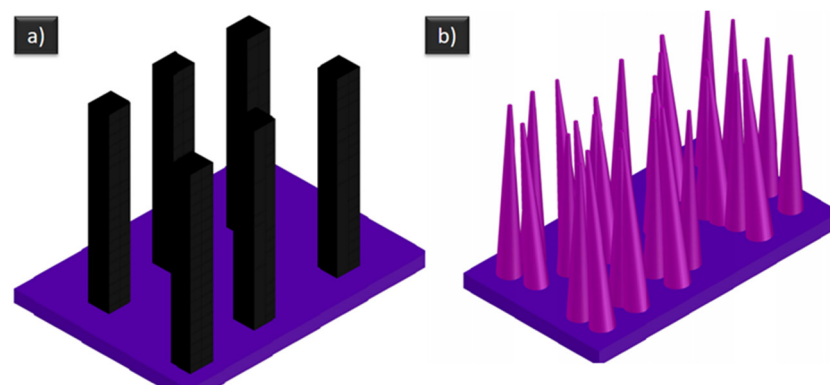


Figure 4. Schematic models of nanostructures reported in the literature: (a) nanorods and (b) nanocones.

2.2.2. Nano-DSSC Structures Higher Efficiency

TiO₂ nanostructures are currently used as photoanode layers in solar cells. These solar cells have achieved excellent results in terms of efficiency. However, not only TiO₂ particles

show this record. The following section reviews articles where high efficiency was reported in the solar cell field. Table 5 describes nanostructures reported with high efficiency values.

Table 5. Nano-DSSC structures higher efficiency.

Idea	Particle	Technique	Structure	η (%)	Ref.
Graphene nanosheets were added to liquid electrolytes to improve the efficiency of DSSCs.	Graphene	-	Nanoleaves	9.26	[9]
Photo anodes composed of a bottom layer of common TiO ₂ nanoparticles and as a top layer one- and three-dimensional TiO _{3,5} nanostructures	TiO ₂	Doctor blading	Nanowires	9.9	[60]
			Core-shell microsphere	9.2	
New method to prepare photoelectrodes incorporating locally ordered 3D-IO TiO ₂ nanostructures.	TiO ₂	New method	Reverse Opal	10.35	[61]
An electrochemical deposition sequenced by an ultrasonic spray coating process is adapted for MoS ₂ /SWCNHs (single-walled carbon nanohorns) bilayer films.	MoS ₂	Electroplating	Nanohorns	9.48	[63]
Co ²⁺ addition in pristine dye-sensitized BaSnO ₃ nanostructures improving energy conversion efficiency	BaSnO ₃	Coprecipitation	Cubic crystalline structure of perovskite	8.22	[7]

As seen in Table 2, reference [60,61] report that using doctor blading techniques and achieve a 9.9% and 9.2% efficiency, respectively. The second reference [61] demonstrates 10.35% efficiency by a new method to prepare photoelectrodes which consist of incorporating locally nanostructures, calcination and etching. If compared to a traditional DSSC, the output performance is significantly better.

There are other types of particles that can be used as nanostructures to improve the efficiency of DSSCs. Such is the case of [9], where graphene nanosheets are added to electrolytes to increase their electrical conductivity and, thus, improve the efficiency of DSSCs. In this work, they report an efficiency of 9.26%. Although this work uses TiO₂ nanoparticles, the nanostructure presented is graphene. In this same work, a comparison between the amount of graphene used (10, 20, and 30 mg) is presented, the amount of 20 mg being the one that showed better results.

In paper [63], the use of molybdenum disulfide for the development of a bilayer counter electrode is presented, where, by means of the electrodeposition technique, the MoS₂ film is grown. Performance is further improved by using SWCNH sputtering, obtaining an efficiency of 9.48%. If compared with the result of only using MoS₂, which was 6.2%, a significant improvement is noticed.

To conclude this section, article [7] reported an efficiency of 8.22% recorded in the solar cell; this was achieved by the precipitation method, adding Co²⁺ to a barium stannate (BaSnO₃) nanostructure. In contrast, it was reported that with 90 mL of SiO₂, desirable core-shell nanoparticles can be formed. Furthermore, an addition of below 90 mL results in a partially bare core, while above 90 mL creates agglomerations and uneven core-shell distribution.

In the scientific literature, there is considerable research on nanostructures. Therefore, outputs can vary from excellent to poor results. Nevertheless, the low efficiency reported in the state of the art serves as a foundation for future research. Table 6 shows articles concerning nanostructures.

Table 6. Nonconventional nanostructures in DSSC.

Particle	Structure	Technique	V _{oc} (V)	η (%)	FF (%)	Ref.
Bi ₂ Ti ₂ O ₇	-	Coprecipitation	721 mV	3.88	54.0	[1]
ZnO:Li	Scale	Hydrothermal	0.64 V	5.58	42.8	[2]
Cu-doped ZnO	Hexagonal wurtzite structure	Coprecipitation	0.64 V	1.34	68.6	[4]
CoS	Nanoflower-shaped star anise structure	Hydrothermal	0.535 V	5.70	63.6	[6]
ZnO doped Li	Nano flowers	Microwave Assisted hydrothermal	0.67 V	1.23	44.0	[8]
Ru _{81.09} Co _{18.91}	-		0.66 V	4.57	49.0	
Ru _{80.55} Se _{19.45}	-	Electroplating	0.64 V	3.82	43.0	[64]
Co _{20.85} Se _{79.15}	-		0.71 V	7.08	62.0	
Fe ₂ O ₃	Nanotubes	Doctor blading	0.68 V	4.0	50.0	[65]
Nitrogen and silver codoped ZnO	Nanowires	Chemical solution	0.631 V	5.10	41.2	[66]
Cu polypyrrole multiwall carbon nanotubes	Nanotubes	Electrodeposition	0.72 V	7.1	69.6	[67]

Contrasting the idea that there are other functional elements in DSSCs besides TiO₂, the use of Bi₂Ti₂O₇(BTO) nanoparticles is presented in the paper [1], showing an efficiency of 3.88%. This research aimed to improve the energy conversion efficiency of the piezo-photo-activated chitosan-based electrolyte for BTO nanoparticles doped with rare and pristine earth. Some of the rare earth elements (REEs) used in this research are samarium (Sm), europium (Eu), erbium (Er), and gadolinium (Gd), among others; it should be noted that REEs were used at 2%. This paper states that the addition of Gd reduces particle size by five times; this presents the best efficiency, which corresponds to the one shown in this review.

In contrast, a study [2] reports efficiency improvement (5.58%) with the incorporation of lithium (Li) to 2D zinc oxide (ZnO) nanostructures. Nevertheless, this paper demonstrates that the addition of Li to the nanostructure reduces resistance to charge transfer and, consequently, efficiency improves. The method used in this article is a hydrothermal method that results in a flake-like structure. In the sense of doping zinc oxide (ZnO) nanostructures, paper [4] presents the doping of this nanostructure using copper (Cu), showing an efficiency of 1.34%. For research purposes, the doping was performed in different proportions (1%, 3%, and 5%). However, only the result for doping at 3% is presented, which, in terms of efficiency, was the best result. In addition, investigators reported that ZnO nanoparticles doped with Cu exhibit localized surface plasmon resonances. Additionally, the optical absorption properties of ZnO were considerably enhanced.

Paper [6] reports the use of cobalt sulfide (CoS) hierarchical nanostructures with an efficiency of 5.7%. The above is achieved using a hydrothermal method and resulted in a star anise nanostructure in the form of a nanoflower. In this research, the authors make a comparison between cobalt sulfide and platinum using the synthetic dye N719. Finally, it was concluded that platinum presented a better efficiency with 6.446%.

Concerning doped zinc oxide (ZnO) nanostructures, two more ideas on this topic are shown in this section; these ideas originated from articles [8,66]. In [8], lithium (Li) is used as a dopant for ZnO nanostructure; the microwave-assisted hydrothermal method is used to synthesize the Li-doped ZnO nanopowders, showing an efficiency of 1.23%. In contrast, they report that the Li-doped ZnO powders have a highly crystalline hexagonal structure and these same nanopowders show a nanoflower morphology. In addition, reference [66]

uses nitrogen and silver as dopants for ZnO. These dopants were used separately and in sets using different proportions of silver. Five models were developed: the first one was without dopants; the second one shows 5% nitrogen; for the third one, 5% of each of the dopants was placed; the fourth one was formed of 5% nitrogen and 10% silver; and finally, the fifth one contained 5% nitrogen and 15% silver. Concerning its efficiency results, the fourth model exhibited the highest efficiency percentage (4.0%). It should be noted that for this research, the chemical solution method was applied using urea as a source of nitrogen.

By using the electrodeposition method in [64], the implementation of different nanostructures based on binary alloys such as $\text{Ru}_{81.09}\text{Co}_{18.91}$, $\text{Ru}_{80.55}\text{Se}_{19.45}$, and $\text{Co}_{20.85}\text{Se}_{79.15}$ is reported. In this work, these alloys were investigated in addition to the performance of the separate elements (Ru, Se, and Co), showing a high efficiency of these alloys. The alloy with the highest efficiency was $\text{Co}_{20.85}\text{Se}_{79.15}$ with 7.08%. As for the tests carried out on each element, ruthenium (Ru) showed an efficiency of 3.22%, selenium (Se) showed an efficiency of 0.34% and finally, cobalt (Co) showed an efficiency of 0.27%.

To conclude this section, reference [65] presents the use of iron oxide (Fe_2O_3) with several porous nanostructures. These nanostructures were synthesized by $\text{Fe}(\text{NO}_3)_3$ /polyvinylpyrrolidone electrospinning followed by calcination in air. Three different types of nanostructures were presented (nanorods, nanotubes, and nanobelts), and the most efficient was the nanotubes with 4.0%. In contrast, the authors claim that the morphology of Fe_2O_3 could be adjusted by changing the ratio between iron nitrates and the polymer.

2.2.3. Recent New Ideas on Nanostructures for DSSCs

One of the most relevant topics for researchers in this field is nanostructures, since the use of nanoscale materials and their structure has a strong influence on DSSCs' efficiency. This section validates that nanoscale materials and their structure significantly influence the efficiency of DSSCs. Recent developments reported as novel nanostructures in DSSCs and their performance are discussed in Table 7.

Table 7. Novel nanostructures reported for DSSCs.

Nanostructure	Type	FF (%)	V_{oc} (V)	η (%)	Ref.
Ag nanoparticles doped on graphene– $\text{Ba}_2\text{GaInO}_6$	Ag 2%	58.01	0.73 V	7.19	[68]
	Ag 4%	64.17	0.78 V	9.01	
	Ag 6%	69.27	0.79 V	9.90	
S-doped TiO_2 nanofibers are introduced as a photoanode in the DSSC	-	59.0	0.683 V	4.27	[69]
Kinetic combination of TiO_2 nanoparticles co-doped with Cu/S photoanodes	Undoped	60.64	0.70 V	6.37	[70]
	0.3% CuS	65.36	0.71 V	10.44	
	0.5% CuS	64.54	0.74 V	5.31	
Nanoporous NiS film with inverse opal and electrocatalytic structure	Nanoporous NiS	64.0	0.73 V	6.77	[71]
	Flat NiS/FTO	62.0	0.73 V	6.30	
	Flat Pt/FTO	65.0	0.73 V	6.69	
Novel hierarchical TiO_2 composite hierarchical structure (TCS) composed of anatase TiO_2 microspheres and rutile TiO_2 nanobelt framework	-	47.0	0.77 V	6.83	[72]

Silver nanoparticles (Ag) doped with graphene- $\text{Ba}_2\text{GaInO}_6$ (G-BGI@Ag), which were synthesized by a hydrothermal process, were used to improve the counter electrode. This is shown in the paper [68], where three different tests are carried out with different proportions of Ag2%, 4% and 6% respectively. The first test showed an efficiency of 7.19%, the second test yielded a result of 9.01% and the final proportion caused the highest

efficiency of 9.90%. They further report that the great performance of G-BGI@AG was related to the synthetic effect between BGI@AG and graphene.

The use of doping in nanostructures has been used to improve the properties of DSSCs, as shown in paper [69], where TiO₂ nanofibers are doped with sulfur (S) in the photoanode. The anode was fabricated by sol–gel electrospinning of poly(vinyl acetate)/titanium isopropoxide followed by calcination at 500 °C. With this technique and preparation method, an efficiency of 4.27% was achieved.

One of the innovative ideas presenting the best efficiency results in this review can be observed in paper [70], where an improvement in the photoanode using TiO₂ nanoparticles co-doped with copper sulfide (Cu/S) with constant content of 0.05% nonmetallic sulfur and diverse content of 0.1 to 0.5% metallic copper is reported. In this paper, it is shown that the nanoparticles were prepared by the sol–gel method. For this article, four tests were carried out: the first one without doping, which presented an efficiency of 6.37%; the other tests were performed with different percentages of Cu/S (0.1%, 0.3%, and 0.5%) where the highest efficiency registered was 10.44% with 0.3% of Cu/S. As for the highest doping, which was 0.5%, this presented a result of lower efficiency than the undoped test.

Paper [71] reports a nonporous nickel sulfide film with an inverse opal structure and electrocatalytic properties. It is obtained through a template-assisted electrodeposition method. The result achieved is a larger specific surface area and more catalytic sites. For this reason, electrolytic activity increases. In this study, the authors report three results. However, the first result showed the highest efficiency (6.77%) using nanoporous NiS.

As the last point in the novelties of nanostructures in the paper [72], a hierarchical TiO₂ composite composed of anatase TiO₂ microspheres and rutile TiO₂ nanobelt structure by hydrothermal focusing is shown. In this study, an efficiency of 6.83% is reported.

3. More Efficient Innovations

Regarding DSSC technology, the efficiency value is the most important in the literature. Several pieces of research focus on improving these values through diverse approaches. It is worth mentioning that the efficiency value serves to compare different types of cells. In addition, it indicates progress and helps to identify, in an easier way, the approach used to achieve such results. Hence, efficiency values are beneficial for researchers since they have a standard to compare their work. The more efficient innovations are summarized in the Table 8.

Table 8. High efficiency values reported on recent literature.

Innovation	Method	η (%)	Ref.
Ag nanoparticles doped with graphene-Ba ₂ GaInO ₆	Ag 4%	9.01	[68]
	Ag 6%	9.90	
Kinetic combination of TiO ₂ nanoparticles co-doped with Cu/S photoanodes	0.1% CuS	9.05	[70]
	0.3% CuS	10.44	
Polymer gel electrolyte containing binary salts of RbI and tetrahexylammonium iodide (Hex ₄ NI) in combination with TiO ₂ multilayer photoelectrodes	Layer3	7.2	[73]
	Layer4	7.5	
Asymmetric dendrimers with ethylene core as quasi-electrolytes	TiO ₂ /N719/LiI/7/Pt	8.494	[74]
	TiO ₂ /N719/LiI/8/Pt	9.037	
Hydrothermal treatment to synthesize highly water-soluble carbon dots from rosemary leaves	CDs(5%)/TiO ₂	7.32	[75]
	CDs(6%)/TiO ₂	6.79	

Research in different areas of materials has been conducted on the use of carbon structures, such as carbon nanotubes, fullerenes, and graphene. Now, we also see how this trend reached DSSCs [68]; in this work, we report the use of silver nanoparticles (Ag) doped with graphene—Ba₂GaInO—which were synthesized by a hydrothermal method to

improve the counter electrode. Different tests were performed in percentages of Ag (0%, 2%, 4%, and 6%). After performing the tests, it was demonstrated that by adding these nanostructures, higher efficiencies are obtained: for the case of Ag at 2%, an efficiency of 7.19% was obtained; by adding Ag 4%, an efficiency of 9.01% was obtained; and finally, by adding 6% of Ag, an efficiency of 9.90% was obtained, this being the highest. Graphene is used as a dopant material, replacing the semiconductor material. This sets a precedent for future research on alternatives to TiO₂. Reinforcing the above, paper [76] shows the incorporation of an anode with flexible dye, which was fabricated by electrophoretic deposition of the photocatalyst on flexible electrodes. This ZnO-based photocatalyst was modified with graphene oxide (GO) by high-energy milling. On the other hand, and continuing with the idea of carbon, a proposal for carbon extraction from a natural source is presented in [75], where carbon dots in the water are synthesized by hydrothermal treatment from rosemary leaves; these leaves were washed with distilled water, dried at room temperature, and then crushed. After, 1 g of these crushed leaves was added to 100 mL of distilled water and heated at 180 °C for 12 h. The solution obtained was centrifuged at 10,000 rpm for 5 min, then kept in a dark glass container at 4 °C. Carbon dots were added in different proportions (1–6%). As for their efficiency, adding these spots at 5% and 6% showed the highest efficiencies with 7.32% and 6.79%, respectively.

As far as the electrolyte is concerned, it has become increasingly important to find an alternative to liquid electrolytes. Such is the case of using binary salts and tetrahexylammonium iodide in gel form in reference [73]. These investigations bring DSSCs closer to achieving a solid or, at least, a quasi-solid version. Also, an improvement in efficiency is mentioned.

On the other hand, a sol–gel route is adopted for the synthesis of undoped TiO₂ nanoparticles co-doped with copper sulfide (Cu/S) with constant content of 0.05% non-metallic sulfur and diverse content of 0.1 to 0.5% metallic copper. The above is presented in paper [70], and it shows one of the highest efficiencies recorded in this review, which means 10.44% to 0.3% CuS tested.

To conclude this section, we report the synthesis of asymmetric stilbenoid-conjugated dendrimers by Heck and Horner–Wadsworth–Emmons coupling in [74]. In this research, the authors state that the absorption intensity improves with an increase in dendrimer generation. Similarly, in this research, good efficiency results are obtained. This is shown in the first-generation asymmetric dendrimer (sample 8), where an efficiency of 9.037% is perceived.

Novel Features

As has been said throughout this document, the subject of DSSCs has a large field of research still ahead of it, in which studies will continue to be carried out with different components or structures to improve overall performance. In addition, other novelties found in this review are shown and discussed below in Table 9.

Sometimes, the novelties presented by some researchers are out of the context of traditional research of the DSSCs. For example, reference [77] presents a study where authors use clathrinid protein obtained from a cow's brain. This research reported that the protein was deposited on a porous TiO₂ semiconductor at different concentrations (0%, 25%, 50%, and 75%). The highest result in terms of efficiency was 1.465%, which corresponds to a 75% concentration of this protein. In contrast, by not using this protein (0% concentration), an efficiency of 0.047% was obtained. Some of the conclusions that stand out in this research are: the addition of this protein forms amino acids, a higher concentration of this protein indicates a more pronounced absorbance of the transmission rate of the wavenumbers in the wave spectrum in the FTIR spectrum, and the increase in concentration of this protein increases the efficiency of the DSSCs.

Table 9. Recent papers that claim novel ideas on DSSCs.

New Ideas Reported on DSSCs	Type	FF (%)	V _{oc} (V)	η (%)	Ref.
Addition of clathrin protein (cow brain)	Clatrina 0%	23.8	562 mV	0.047	[77]
	Clatrina 50%	31.3	624 mV	0.516	
	Clatrina 75%	42.5	657 mV	1.465	
Compositions of “Bi _x Zn _{1-x} O _y ” have been synthesized by the gel combustion technique of citrate nitrate, with dye N719	BZO 0.02	64.6	0.69 V	0.2	[78]
	BZO 0.04	68.7	0.73 V	0.14	
	BZO 0.06	68.0	0.82 V	0.13	
Binary (CoS, NiS and ZnS) and ternary (CoNiS ₄ and Zn _{0.76} Co _{0.24} S) micro/nanoscale metal sulfides were obtained directly on FTO substrates.	CoS	61.26	0.522 V	2.402	[79]
	NiS	63.07	0.570 V	2.058	
	ZnS	45.15	0.461 V	1.124	
	CoNi ₂ S ₄	66.62	0.538 V	4.037	
	Zn _{0.76} Co _{0.24} S	60.09	0.552 V	3.522	

Paper [78] reports the use of bismuth-doped zinc oxide nanoparticles (Bi_xZn_{1-x}O_y). Preparation included the citrate nitrate gel combustion method, which is a modification of the sol-gel method. In this research, there are three different compositions of zinc oxide doped with bismuth (Bi_{0.02}Zn_{0.98}O_y, Bi_{0.04}Zn_{0.96}O_y, and Bi_{0.06}Zn_{0.94}O_y); the highest efficiency registered is 0.25% and this corresponds to the composition Bi_{0.02}Zn_{0.98}O_y. Finally, the authors used synthetic dye N719 for this research.

Paper [79] reports different binary metallic sulfides being obtained through the sol-gel technique such as carbonyl sulfide (CoS), nickel sulfide (NiS), and zinc sulfide (ZnS). Ternary metal sulfides such as CoNi₂S₄ and Zn_{0.76}Co_{0.24}S were grown in this same study. They report that both binary and ternary metal sulfides were grown directly on FTO substrates by reaction in a hydrothermal reactor and these were used as counter electrodes. As for the efficiency results, the tertiary metal sulfide CoNi₂S₄ showed a percentage of 4.03%, which, as they report, is comparable with a standard efficiency of 4.59%.

4. Conclusions

- ✓ Nanostructure materials continue to enhance energy efficiency conversion. Therefore, it remains a relevant and widely discussed topic throughout this work. Additionally, doped materials are a milestone in efficiency enhancement. Current trends include nanostructure-doped materials due to their high efficiency (TiO₂ nanoparticles co-doped with Cu/S). Therefore, future research on DSSC improvement will involve nanostructure and doping materials. It is worth mentioning that new dyes with natural origins continue to be reported in current trends. Therefore, this published literature emphasizes the interest in finding sensitizers with suitable properties for energy harvesting, as well as a growing interest in low-cost manufacturing methods and environmental performance. In this review, a significant number of articles on natural dyes were included and discussed. Therefore, this review identified the growing use of TiO₂ in DSSCs. Since TiO₂ provides increased stability, and a large amount of research acts as a standard to compare, it has become a popular trend in the field. At present, it is still the most used in the reported literature. However, it is important to clarify that as research progresses, the use of other materials is coming to light, displacing TiO₂ and even almost obtaining values very close to it in terms of efficiency.
- ✓ Current high efficiency values have already been achieved compared to the previous investigation found in the literature. However, DSSC technology has room left for future research and development—particularly, investigation on the stability of conversion values over time. Finally, the possibility of developing DSSCs in a solid state would open a wide field of research and improvement of DSSCs.

Author Contributions: Conceptualization, J.A.C.-R., E.N.A.-M. and J.A.R.-d.-L.; methodology, J.A.C.-R. and E.N.A.-M.; validation, E.R.-R. and J.A.R.-d.-L.; formal analysis, E.N.A.-M. and F.C.C.-R.; investigation, J.A.C.-R., E.N.A.-M.; resources, F.C.C.-R. and J.A.R.-d.-L.; data curation, J.A.C.-R., E.N.A.-M. and E.R.-R.; writing—original draft preparation, J.A.C.-R. and E.N.A.-M.; writing—review and editing, E.N.A.-M. and E.R.-R.; visualization, J.A.R.-d.-L.; supervision, F.C.C.-R.; project administration, E.N.A.-M. All authors have read and agreed to the published version of the manuscript.

Funding: This research received no external funding.

Conflicts of Interest: The authors declare no conflict of interest.

References

1. Praveen, E.; Peter, I.J.; Kumar, A.M.; Ramachandran, K.; Jayakumar, K. Performance of phototronically activated chitosan electrolyte in rare-earth doped $\text{Bi}_2\text{Ti}_2\text{O}_7$ nanostructure based DSSC. *Mater. Lett.* **2020**, *276*, 128202. [[CrossRef](#)]
2. Praveen, E.; Peter, I.J.; Kumar, A.M.; Ramachandran, K.; Jayakumar, K. Boosting of power conversion efficiency of 2D ZnO nanostructures-based DSSC by the Lorentz force with chitosan polymer electrolyte. *J. Inorg. Organomet. Polym. Mater.* **2020**, *30*, 4927–4943. [[CrossRef](#)]
3. Priyono, B.; Yuwono, A.H.; Syahrial, A.Z.; Mustofa, M.H.; Bawono, R.S. Performance of post-hydrothermally treated xerogel TiO_2 dye-sensitized solar cell (DSSC) and its nanostructure characteristic. *Mater. Sci. Eng.* **2018**, *432*, 12–30. [[CrossRef](#)]
4. Aneesiya, K.R.; Louis, C. Localized surface plasmon resonance of Cu-doped ZnO nanostructures and the material's integration in dye sensitized solar cells (DSSCs) enabling high open-circuit potentials. *J. Alloys Compd.* **2020**, *829*, 154497. [[CrossRef](#)]
5. Fadhilah, N.; Pratama, D.Y.; Sawitri, D.; Risanti, D.D. Preparation of Au@TiO₂@SiO₂ core-shell nanostructure and their light harvesting capability on DSSC (dye sensitized solar cells). *AIP Conf. Proc.* **2019**, *2088*, 060007. [[CrossRef](#)]
6. Kumar, K.A.; Pandurangan, A.; Arumugam, S.; Sathiskumar, M. Effect of bi-functional hierarchical flower-like CoS nanostructure on its interfacial charge transport kinetics, magnetic and electrochemical behaviors for supercapacitor and DSSC applications. *Sci. Rep.* **2019**, *9*, 1–16. [[CrossRef](#)]
7. Rajamanickam, N.; Isogami, S.; Ramachandran, K. Effect of Co doping for improved photovoltaic performance of dye-sensitized solar cells in BaSnO_3 nanostructures. *Mater. Lett.* **2020**, *275*, 128139. [[CrossRef](#)]
8. Aksoy, S.; Polat, O.; Gorgun, K.; Caglar, Y.; Caglar, M. Li doped ZnO based DSSC: Characterization and preparation of nanopowders and electrical performance of its DSSC. *Physica E Low-dimensi. Syst. Nanostruct.* **2020**, *121*, 114127. [[CrossRef](#)]
9. Tsai, C.H.; Chuang, P.Y.; Hsu, H.L. Adding graphene nanosheets in liquid electrolytes to improve the efficiency of dye-sensitized solar cells. *Mater. Chem. Phys.* **2018**, *207*, 154–160. [[CrossRef](#)]
10. Cui, Y.; Wang, W.; Li, N.; Ding, R.; Hong, K. Hetero-seed mediated method to synthesize ZnO/TiO₂ multipod nanostructures with ultra-high yield for dye-sensitized solar cells. *J. Alloys Compd.* **2019**, *805*, 868–872. [[CrossRef](#)]
11. Ramakrishnan, V.M.; Muthukumarasamy, N.; Balraju, P.; Pitchaiya, S.; Velauthapillai, D.; Pugazhendhi, A. Transformation of TiO₂ nanoparticles to nanotubes by simple solvothermal route and its performance as dye-sensitized solar cell (DSSC) photoanode. *Int. J. Hydrogen Energy* **2020**, *45*, 15441–15452. [[CrossRef](#)]
12. Shalini, S.; Balasundaraprabhu, R.; Kumar, T.S.; Sivakumaran, K.; Kannan, M.D. Synergistic effect of sodium and yeast in improving the efficiency of DSSC sensitized with extract from petals of *Kigelia Africana*. *Opt. Mater.* **2018**, *79*, 210–219. [[CrossRef](#)]
13. Shalini, S.; Kumar, T.S.; Prasanna, S.; Balasundaraprabhu, R. Investigations on the effect of co-doping in enhancing the performance of nanostructured TiO₂ based DSSC sensitized using extracts of *Hibiscus Sabdariffa* calyx. *Optik* **2020**, *212*, 164672. [[CrossRef](#)]
14. Sinha, D.; De, D.; Goswami, D.; Ayaz, A. Fabrication of DSSC with nanostructured ZnO photo anode and natural dye sensitizer. *Mater. Today* **2018**, *5*, 2056–2063. [[CrossRef](#)]
15. Bashar, H.; Bhuiyan, M.M.H.; Hossain, M.R.; Kabir, F.; Rahaman, M.S.; Manir, M.S.; Ikegami, T. Study on combination of natural red and green dyes to improve the power conversion efficiency of dye sensitized solar cells. *Optik* **2019**, *185*, 620–625. [[CrossRef](#)]
16. Kabir, F.; Bhuiyan, M.M.H.; Manir, M.S.; Rahaman, M.S.; Khan, M.A.; Ikegami, T. Development of dye-sensitized solar cells based on a combination of natural dyes extracted from Malabar spinach and red spinach. *Results Phys.* **2019**, *14*, 102474. [[CrossRef](#)]
17. Maurya, I.C.; Singh, S.; Srivastava, P.; Maiti, B.; Bahadur, L. Natural dye extract from *Cassia fistula* and its application in dye-sensitized solar cells: Experimental and density functional theory studies. *Opt. Mater.* **2019**, *90*, 273–280. [[CrossRef](#)]
18. Ammar, A.M.; Mohamed, H.S.; Yousef, M.M.; Abdel-Hafez, G.M.; Hassaniien, A.S.; Khalil, A.S. Dye-sensitized solar cells (DSSCs) based on extracted natural dyes. *J. Nanomater.* **2019**, *1*, 2019. [[CrossRef](#)]
19. Kocak, Y.; Atli, A.; Atilgan, A.; Yildiz, A. Extraction method dependent performance of bio-based dye-sensitized solar cells (DSSCs). *Mater. Res. Express* **2019**, *6*, 095512. [[CrossRef](#)]
20. Atli, A.; Atilgan, A.; Altinkaya, C.; Ozel, K.; Yildiz, A. St. Lucie cherry, yellow jasmine, and madder berries as novel natural sensitizers for dye-sensitized solar cells. *Int. J. Energy Res.* **2019**, *43*, 3914–3922. [[CrossRef](#)]
21. Jalali, T.; Arkian, P.; Golshan, M.; Jalali, M.; Osfouri, S. Performance evaluation of natural native dyes as photosensitizer in dye-sensitized solar cells. *Opt. Mater.* **2020**, *110*, 110441. [[CrossRef](#)]
22. Najm, A.S.; Ludin, N.A.; Abdullah, M.F.; Almessiere, M.A.; Ahmed, N.M.; Al-Alwani, M.A. Areca catechu extracted a natural new sensitizer for dye-sensitized solar cells: Performance evaluation. *J. Mater. Sci. Mater. Electron.* **2020**, *31*, 3564–3575. [[CrossRef](#)]

23. Pratiwi, D.D.; Nurosyid, F.; Supriyanto, A.; Suryana, R. Efficiency enhancement of dye-sensitized solar cells (DSSC) by addition of synthetic dye into natural dye (anthocyanin). *IOP Conf. Ser. Mater. Sci. Eng.* **2017**, *176*, 012012. [[CrossRef](#)]
24. Ruhane, T.A.; Islam, M.T.; Rahaman, M.S.; Bhuiyan, M.M.H.; Islam, J.M.; Newaz, M.K.; Khan, M.A. Photo current enhancement of natural dye sensitized solar cells by optimizing dye extraction and its loading period. *Optik* **2017**, *149*, 174–183. [[CrossRef](#)]
25. Güzel, E.; Arslan, B.S.; Durmaz, V.; Cesur, M.; Tutar, Ö.F.; Sarı, T.; Şişman, İ. Photovoltaic performance and photostability of anthocyanins, isoquinoline alkaloids and betalains as natural sensitizers for DSSCs. *Sol. Energy* **2018**, *173*, 34–41. [[CrossRef](#)]
26. Sampaio, D.M.; Babu, R.S.; Costa, H.; de Barros, A. Investigation of nanostructured TiO₂ thin film coatings for DSSCs application using natural dye extracted from jaboticaba fruit as photosensitizers. *Ionics* **2019**, *25*, 2893–2902. [[CrossRef](#)]
27. Al-Alwani, M.A.; Ludin, N.A.; Mohamad, A.B.; Kadhum, A.; Mukhlus, A. Application of dyes extracted from *Alternanthera dentata* leaves and *Musa acuminata* bracts as natural sensitizers for dye-sensitized solar cells. *Spectrochim. Acta A Mol. Biomol. Spectrosc.* **2018**, *192*, 487–498. [[CrossRef](#)]
28. Arifin, Z.; Soeparman, S.; Widhiyanuriyawan, D.; Suyitno, S.; Setyaji, A.T. Improving stability of chlorophyll as natural dye for dye-sensitized solar cells. *J. Teknol.* **2018**, *80*, 27–33. [[CrossRef](#)]
29. Bachtiar, M.I.; Agustina, M.N.P.; Hariyani, L.W.; Nurosyid, F. Effect of dye variation on DSSC efficiency. *J. Phys. Conf. Ser.* **2019**, *1153*, 012097. [[CrossRef](#)]
30. Madnasri, S.; Wulandari, R.D.A.; Hadi, S.; Yulianti, I.; Edi, S.S.; Prastiyanto, D. Natural Dye of *Musa acuminata* bracts as Light Absorbing Sensitizer for Dye-Sensitized Solar Cell. *Mater. Today* **2019**, *13*, 246–251. [[CrossRef](#)]
31. Ismail, M.; Ludin, N.A.; Hamid, N.H.; Ibrahim, M.A.; Sopian, K. The effect of chenodeoxycholic acid (CDCA) in Mangosteen (*Garcinia mangostana*) pericarps sensitizer for dye-sensitized solar cell (DSSC). *J. Phys. Conf. Ser.* **2018**, *1083*, 012018. [[CrossRef](#)]
32. Kabir, F.; Bhuiyan, M.; Hossain, M.R.; Bashar, H.; Rahaman, M.S.; Manir, M.S.; Khan, M.A. Improvement of efficiency of dye sensitized solar cells by optimizing the combination ratio of natural red and yellow dyes. *Optik* **2019**, *179*, 252–258. [[CrossRef](#)]
33. Diantoro, M.; Maftuha, D.; Suprayogi, T.; Iqbal, M.R.; Mufti, N.; Taufiq, A.; Hidayat, R. Performance of *Pterocarpus Indicus* Willd Leaf Extract as Natural Dye TiO₂-Dye/ITO DSSC. *Mater. Today* **2019**, *17*, 1268–1276. [[CrossRef](#)]
34. Tahir, D.; Satriani, W.; Gareso, P.L.; Abdullah, B. Dye sensitized solar cells (DSSC) with natural dyes extracted from *Jatropha* leaves and purple *Chrysanthemum* flowers as sensitizer. *J. Phys. Conf. Ser.* **2018**, *979*, 012056. [[CrossRef](#)]
35. Sinha, D.; De, D.; Ayaz, A. Photo sensitizing and electrochemical performance analysis of mixed natural dye and nanostructured ZnO based DSSC. *Sādhanā* **2020**, *45*, 1–12. [[CrossRef](#)]
36. Oktariza, L.G.; Yulianto, B.; Suyatman. Performance of dye sensitized solar cells (DSSC) using *Syngonium Podophyllum* Schott as natural dye and counter electrode. *AIP Conf. Proc.* **2018**, *1958*, 020022. [[CrossRef](#)]
37. Hamid, N.; Suhaimi, S.; Yatim, N.M. Effect of natural dye sensitizers towards the improvement of dye-sensitized solar cell (DSSC) efficiency. *AIP Conf. Proc.* **2018**, *1972*, 030009. [[CrossRef](#)]
38. Erande, K.B.; Hawaldar, P.Y.; Suryawanshi, S.R.; Babar, B.M.; Mohite, A.A.; Shelke, H.D.; Pawar, U.T. Extraction of natural dye (specifically anthocyanin) from pomegranate fruit source and their subsequent use in DSSC. *Mater. Today* **2020**, *43*, 2716–2720. [[CrossRef](#)]
39. Lohar, G.M.; Rupnawar, D.V.; Shejawal, R.V.; Fulari, A.V. Preparation of natural dyes from *salvia* and *spathodea* for TiO₂-based dye-sensitized solar cells (DSSCs) and their electrochemical impedance spectroscopic study under light and dark conditions. *Bull. Mater. Sci.* **2020**, *43*, 1–8. [[CrossRef](#)]
40. Supriyanto, A.; Cari, C.; Suciati, P.M.; Kurniawan, D.; Septiawan, T.Y. The fabrication of DSSC TiO₂ transparent thin layer with natural dye sweet potato (*Ipomoea batatas* L.). *J. Phys. Conf. Ser.* **2019**, *1153*, 012098. [[CrossRef](#)]
41. Pathak, C.; Surana, K.; Shukla, V.K.; Singh, P.K. Fabrication and characterization of dye sensitized solar cell using natural dyes. *Mater. Today* **2019**, *12*, 665–670. [[CrossRef](#)]
42. Leyrer, J.; Rubilar, M.; Morales, E.; Pavez, B.; Leal, E.; Hunter, R. Factor optimization in the manufacturing process of dye-sensitized solar cells based on naturally extracted dye from a Maqui and blackberry mixture (*Aristotelia chilensis* and *Rubus glaucus*). *J. Electron. Mater.* **2018**, *47*, 6136–6143. [[CrossRef](#)]
43. Hafez, H.S.; Shenouda, S.S.; Fadel, M. Photovoltaic characteristics of natural light harvesting dye sensitized solar cells. *Spectrochim. Acta A Mol. Biomol. Spectrosc.* **2018**, *192*, 23–26. [[CrossRef](#)]
44. Faraz, S.M.; Mazhar, M.; Shah, W.; Noor, H.; Awan, Z.H.; Sayyad, M.H. Comparative study of impedance spectroscopy and photovoltaic properties of metallic and natural dye based dye sensitized solar cells. *Phys. B Condens. Matter* **2021**, *602*, 412567. [[CrossRef](#)]
45. Kiran, S.; Ramesh, T.; Murthy, S.R. Preparation and characterization of (100 – x) TiO₂ + (x)ZnO nanocomposites for dye-sensitized solar cells using *Beta vulgaris* and *Syzygium cumini* natural dye extract. *J. Mater. Sci. Mater. Electron.* **2018**, *29*, 11712–11718. [[CrossRef](#)]
46. Jun, H.K.; Arof, A.K. Performance of natural dyes as sensitizer in dye-sensitized solar cells employing LiBOB-based liquid electrolyte. *Ionics* **2018**, *24*, 915–922. [[CrossRef](#)]
47. Golshan, M.; Osfouri, S.; Azin, R.; Jalali, T. Fabrication of optimized eco-friendly dye-sensitized solar cells by extracting pigments from low-cost native wild plants. *J. Photochem. Photobiol. A Chem.* **2020**, *388*, 112191. [[CrossRef](#)]
48. Devi, S.B.; Babu, D.P.; Kumar, S.N.; Bindu, P.K. Influence of different natural dyes as sensitizers on the performance of DSSCs. *AIP Conf. Proc.* **2020**, *2244*, 110012. [[CrossRef](#)]

49. Orona-Navar, A.; Aguilar-Hernández, I.; López-Luke, T.; Zarazúa, I.; Romero-Arellano, V.; Guerrero, J.P.; Ornelas-Soto, N. Photoconversion efficiency of Titania solar cells co-sensitized with natural pigments from cochineal, papaya peel and microalga *Scenedesmus obliquus*. *J. Photochem. Photobiol. A Chem.* **2020**, *388*, 112216. [[CrossRef](#)]
50. Adedokun, O.; Adedeji, O.L.; Awodele, M.K.; Bello, I.T.; Awodugba, A.O. Citrus fruit peels extracts as light harvesters for efficient ZnO-based dye-sensitized solar cells. *J. Phys. Conf. Ser.* **2019**, *1299*, 012010. [[CrossRef](#)]
51. Purushothamreddy, N.; Dileep, R.K.; Veerappan, G.; Kovendhan, M.; Joseph, D.P. Prickly pear fruit extract as photosensitizer for dye-sensitized solar cell. *Spectrochim. Acta A Mol. Biomol. Spectrosc.* **2020**, *228*, 117686. [[CrossRef](#)]
52. Supriyanto, A.; Nurosyid, F.; Ahliha, A.H. Carotenoid pigment as sensitizers for applications of dye-sensitized solar cell (DSSC). *IOP Conf. Ser. Mater. Sci. Eng.* **2018**, *432*, 012060. [[CrossRef](#)]
53. Diyanahesa, N.E.H.; Supriyanto, A.; Ramelan, A.H. Improvement of efficiency of dye-sensitized solar cells (DSSC) transparent by optimizing anthocyanin dyes hybrid dyenamo yellow (DN-F01). *AIP Conf. Proc.* **2020**, *2217*, 030182. [[CrossRef](#)]
54. Arslan, B.S.; Güzel, E.; Kaya, T.; Durmaz, V.; Keskin, M.; Avcı, D.; Şişman, İ. Novel D- π -A organic dyes for DSSCs based on dibenzo [b, h][1,6] naphthyridine as a π -bridge. *Dyes Pigment.* **2019**, *164*, 188–197. [[CrossRef](#)]
55. Jadhav, M.M.; Chowdhury, T.H.; Bedja, I.; Patil, D.; Islam, A.; Sekar, N. Near IR emitting novel rhodanine-3-acetic acid based two donor- π -acceptor sensitizers for DSSC: Synthesis and application. *Dyes Pigment.* **2019**, *165*, 391–399. [[CrossRef](#)]
56. Jadhav, M.M.; Vaghasiya, J.V.; Patil, D.; Soni, S.S.; Sekar, N. Synthesis of novel colorants for DSSC to study effect of alkyl chain length alteration of auxiliary donor on light to current conversion efficiency. *J. Photochem. Photobiol. A Chem.* **2019**, *377*, 119–129. [[CrossRef](#)]
57. Seyednoruziyan, B.; Zamanloo, M.R.; Shamkhali, A.N.; Alizadeh, T.; Noruzi, S.; Aslani, S. Improving the optoelectronic efficiency of novel meta-azo dye-sensitized TiO₂ semiconductor for DSSCs. *Spectrochim. Acta A Mol. Biomol. Spectrosc.* **2021**, *247*, 119143. [[CrossRef](#)] [[PubMed](#)]
58. Duerto, I.; Barrios, D.; Garín, J.; Orduna, J.; Villacampa, B.; Blesa, M.J. Difunctionalized dyes for DSSCs based on two different scaffolds: P-tert-butylcalix[4]arene or isophthalic acid. *Dyes Pigment.* **2020**, *182*, 108530. [[CrossRef](#)]
59. Lyu, L.; Su, R.; Al-Qaradawi, S.Y.; Al-Saad, K.A.; El-Shafei, A. Three-component one-pot reaction for molecular engineering of novel cost-effective highly rigid quinoxaline-based photosensitizers for highly efficient DSSCs application: Remarkable photovoltage. *Dyes Pigment.* **2019**, *171*, 107683. [[CrossRef](#)]
60. Balu, M.; Baiju, K.G.; Subramaniam, M.R.; Kumaresan, D. Bi-layer photoanodes with superior charge collection ability and diffusion length of sub-layer nanostructures for the fabrication of high efficiency dye-sensitized solar cells. *Electrochim. Acta* **2019**, *319*, 339–348. [[CrossRef](#)]
61. Xu, L.; Aumaitre, C.; Kervella, Y.; Lapertot, G.; Rodríguez-Seco, C.; Palomares, E.; Reiss, P. Increasing the Efficiency of Organic Dye-Sensitized Solar Cells over 10.3% Using Locally Ordered Inverse Opal Nanostructures in the Photoelectrode. *Adv. Funct. Mater.* **2018**, *28*, 1706291. [[CrossRef](#)]
62. Yin, X.; Guan, Y.; Song, L.; Xie, X.; Du, P.; Xiong, J. The TiO₂ Hierarchical Structure with Nanosheet Spheres for Improved Photoelectric Performance in Dye-Sensitized Solar Cells. *J. Electron. Mater.* **2018**, *47*, 2230–2236. [[CrossRef](#)]
63. Gurulakshmi, M.; Meenakshamma, A.; Susmitha, K.; Venkata Subbaiah, Y.P.; Mitty, R. Enhanced Performance of Dye-Sensitized Solar Cells (DSSCs) Based on MoS₂/Single-Walled Carbon Nanohorns Electrochemically Deposited on Bilayer Counter Electrodes. *ChemPlusChem* **2020**, *85*, 2599–2605. [[CrossRef](#)]
64. Liu, W.W.; Jiang, W.; Liu, Y.C.; Niu, W.J.; Liu, M.C.; Kong, L.B.; Chueh, Y.L. Interface engineered Binary platinum free Alloy-based counter electrodes with improved performance in Dye-Sensitized Solar cells. *Sci. Rep.* **2020**, *10*, 1–12. [[CrossRef](#)]
65. Zhang, C.; Zhang, P.; Zhang, H. Electrospun porous Fe₂O₃ nanotubes as counter electrodes for dye-sensitized solar cells. *Int. J. Energy Res.* **2019**, *43*, 5355–5366. [[CrossRef](#)]
66. Kumari, M.; Kundu, V.S.; Kumar, S.; Siwach, S.; Chauhan, N. Nitrogen and silver co-doped one-dimensional ZnO nanostructure for optoelectronic application. *J. Sol-Gel Sci. Tech.* **2020**, *93*, 302–308. [[CrossRef](#)]
67. Rafique, S.; Rashid, I.; Sharif, R. Cost effective dye sensitized solar cell based on novel Cu polypyrrole multiwall carbon nanotubes nanocomposites counter electrode. *Sci. Rep.* **2021**, *11*, 1–8. [[CrossRef](#)]
68. Oh, W.C.; Chanthai, S.; Areerob, Y. Novel flexible Ag nanoparticles doped on graphene–Ba₂GaInO₆ as cathode material for enhancement in the power conversion of DSSCs. *Sol. Energy* **2019**, *180*, 510–518. [[CrossRef](#)]
69. Mahmoud, M.S.; Akhtar, M.S.; Mohamed, I.M.; Hamdan, R.; Dakka, Y.A.; Barakat, N.A. Demonstrated photons to electron activity of S-doped TiO₂ nanofibers as photoanode in the DSSC. *Mater. Lett.* **2018**, *225*, 77–81. [[CrossRef](#)]
70. Gupta, A.; Sahu, K.; Dhonde, M.; Murty, V. Novel synergistic combination of Cu/S co-doped TiO₂ nanoparticles incorporated as photoanode in dye sensitized solar cell. *Sol. Energy* **2020**, *203*, 296–303. [[CrossRef](#)]
71. Chen, X.; Zhang, Y.; Pang, Y.; Jiang, Q. Facile Synthesis of Nanoporous NiS Film with Inverse Opal Structure as Efficient Counter Electrode for DSSCs. *Materials* **2020**, *13*, 4647. [[CrossRef](#)]
72. Zhao, F.; Ma, R.; Jiang, Y. Strong efficiency improvement in dye-sensitized solar cells by novel multi-dimensional TiO₂ photoelectrode. *Appl. Surf. Sci.* **2018**, *434*, 11–15. [[CrossRef](#)]
73. Bandara, T.; DeSilva, L.A.; Ratnasekera, J.L.; Hettiarachchi, K.H.; Wijerathna, A.P.; Thakurdesai, M.; Mellander, B.E. High efficiency dye-sensitized solar cell based on a novel gel polymer electrolyte containing RbI and tetrahexylammonium iodide (Hex₄NI) salts and multi-layered photoelectrodes of TiO₂ nanoparticles. *Renew. Sustain. Energy Rev.* **2019**, *103*, 282–290. [[CrossRef](#)]

74. Ravivarma, M.; Kumar, K.A.; Rajakumar, P.; Pandurangan, A. Interfacial charge transport studies and fabrication of high performance DSSC with ethylene cored unsymmetrical dendrimers as quasi electrolytes. *J. Mol. Liq.* **2018**, *265*, 717–726. [[CrossRef](#)]
75. Rezaei, B.; Irannejad, N.; Ensafi, A.A.; Kazemifard, N. The impressive effect of eco-friendly carbon dots on improving the performance of dye-sensitized solar cells. *Sol. Energy.* **2019**, *182*, 412–419. [[CrossRef](#)]
76. Atanacio-Sánchez, X.; Pech-Rodríguez, W.J.; Armendáriz-Mireles, E.N. Improving performance of ZnO flexible dye sensitized solar cell by incorporation of graphene oxide. *Microsyst. Technol.* **2020**, *26*, 3591–3599. [[CrossRef](#)]
77. Widhiyanuriyawan, D.; Trihutomo, P.; Soeparman, S.; Yuliati, L. Zwitterion Effect of Cow Brain Protein towards Efficiency Improvement of Dye-Sensitized Solar Cell (DSSC). *Sci. World J.* **2020**, *2020*, 1–12. [[CrossRef](#)]
78. Fatima, M.J.; Niveditha, C.V.; Sindhu, S. Novel Bi₂O₃-ZnO solid solutions as photoanode in DSSC. *AIP Conf. Proc.* **2019**, *2082*, 050003. [[CrossRef](#)]
79. Subalakshmi, K.; Kumar, K.A.; Paul, O.P.; Saraswathy, S.; Pandurangan, A.; Senthilselvan, J. Platinum-free metal sulfide counter electrodes for DSSC applications: Structural, electrochemical and power conversion efficiency analyses. *Sol. Energy* **2019**, *193*, 507–518. [[CrossRef](#)]